



Contents lists available at ScienceDirect

Journal of Computational and Applied Mathematics

journal homepage: www.elsevier.com/locate/cam

Spline spaces with mixed orders of continuity over T-meshes



Meng Wu^{a,b,c}, Weihong Zhang^{a,d}, Zhouwang Yang^a, Jiansong Deng^{a,*},
Falai Chen^a

^a School of Mathematical Sciences, University of Science and Technology of China, Hefei, Anhui, 230026, PR China

^b Galaad, INRIA Sophia-Antipolis, 2004 Route des Lucioles, 06902 Cedex, France

^c University of Nice Sophia-Antipolis, 06108 Nice Cedex 02, France

^d Hefei Normal University, Hefei, Anhui, 230026, PR China

HIGHLIGHTS

- A concept “Spline spaces with mixed orders of continuity over T-meshes” is presented.
- Dimensional formulas are given for this type of bicubic spline spaces.
- A set of bases are constructed with nice property from the geometric view.
- Applications in image processing and FEM are presented.

ARTICLE INFO

Article history:

Received 3 April 2013

Received in revised form 26 February 2014

Keywords:

Spline

T-mesh

Discontinuous data processing

Finite element method

B-net method

ABSTRACT

In this paper, we introduce the concept of spline spaces with mixed orders of continuity over T-meshes. Then, the dimensions of the cubic spline spaces with continuity of order one and locally discontinuous over hierarchical T-meshes are presented by the B-net method. From the viewpoint of processing geometry data, a non-negative basis set with local support and partition of unity is constructed. Finally, the behavior of this type of spline is analyzed with the help of examples in image processing and finite element analysis.

© 2014 Elsevier B.V. All rights reserved.

1. Introduction

Spline functions are well-known functions that are defined by piecewise polynomials and whose study was first reported in [1] in 1946. A B-spline function is a type of spline and that forms natural basis functions of univariate spline spaces. Due to its computational feasibility, B-spline functions are widely used in computer aided geometric design, data processing, numerical computing [2,3], etc. Spline theory is closely related to optimal control, statistics [4] and geometric computing [5].

To describe multivariate data, the tensor products of B-splines are introduced. A serious weakness of tensor-product splines is that they contain a large number of superfluous control points. To reduce the number of these superfluous control points, several different types of splines defined over T-meshes are constructed, such as hierarchical B-splines [6], T-splines [7] and spline spaces over T-meshes [8], where a T-mesh is a rectangular grid that allows T-junctions [7].

When traditional spline functions are used to handle discontinuous data, the data is considered to lie on a surface with uniform global smoothness because a traditional bivariate spline function has the same order of continuity along the x-direction and the y-direction everywhere. However, this assumption is not always reasonable. For example, from the view

* Corresponding author.

E-mail address: dengjs@ustc.edu.cn (J. Deng).

of human vision, the boundary of an object represents important information that distinguishes the object from its background. In image processing, if we use smooth splines to handle this object and its background, the object's boundary must be blurred and this object may even be lost if it is small. Moreover, there is a Gibbs phenomenon for smooth splines [9], when these smooth splines are used to deal with discontinuous data.

Discontinuity is a feature of such natural phenomenon in the world as shock waves, phase transitions and digital signals. In approximation theory and finite element analysis, there are some methods that have been developed to address discontinuity problems. For example, in approximation theory, there are some function systems for handling discontinuous data, such as the Walsh function system [10] and Haar function system [11], which are well known in signal processing and image analysis. More recently, the U-system [12] and V-system [13] generalized the aforementioned function systems to a higher degree. In terms of spline theory, the U-system and V-system are univariate splines of degree k with continuity of order -1 on a knot sequence. There are some disadvantages to using C^{-1} splines to handle discontinuous problems, such as lower computing efficiency due to redundant basis functions or shape functions. Moreover, C^{-1} splines lead to discontinuity over smooth parts. In finite element analysis, the discontinuous Galerkin (DG) method is a famous technique for solving PDEs with completely discontinuous piecewise polynomial (C^{-1} -splines) space for the numerical solution and the test functions. There are many papers on DG, for example, the review [14]. If a PDE has a smoothness solution, a “numerical flux” is introduced into the DG method in order to prevent the problems caused by using C^{-1} -splines.

In addition to C^{-1} splines, R. H. Wang proposed the concept of spline spaces with mixed orders of continuity over arbitrary triangular partitions in [15] in 1979 to describe discontinuous phenomena. In the present paper, based on spline spaces over T-meshes [16,8], we propose the concept of spline spaces with mixed orders of continuity over T-meshes and provide dimensional formulae for these spaces of bicubic splines with continuity of order 1 or -1 over hierarchical T-meshes called combined PHT (C-PHT). We also construct a set of basis functions with important properties such as non-negativity, local support and partition of unity for the space of special C-PHT.

The remainder of the paper is organized as follows. In Section 2, the concept of spline spaces with mixed orders of continuity over T-meshes is proposed. In particular, C-PHT is treated as a special case. Then, the dimensional formula of the space of C-PHT is presented in Section 3, and a set of basis functions is constructed by the B-net method [8] in Section 4. In Section 5, some examples of the use of C-PHT in image processing and to solve PDEs are presented. After analyzing these examples, conclusions and future research problems are presented in Section 6.

2. Spline spaces with mixed orders of continuity over T-meshes

In this section, we first review a few concepts regarding T-meshes and spline spaces over T-meshes. Then, we present the concepts of spline spaces with mixed orders of continuity over T-meshes and combined PHT (C-PHT for short).

2.1. T-meshes and spline spaces over T-meshes

To reduce the superfluous degrees of freedom of splines defined over tensor product meshes, T-meshes are introduced. A hierarchical T-mesh is a type of T-meshes with a natural level structure [16]. In the following, we will introduce some concepts.

A T-mesh \mathcal{T} [17] is a set of axis-aligned rectangles, and the intersection of any two distinct rectangles in \mathcal{T} is either empty or consists of points on the boundaries of the rectangles. Moreover, if the entire domain occupied by \mathcal{T} is a rectangle, \mathcal{T} is called a regular T-mesh, otherwise, it is irregular. There are two T-meshes shown in Fig. 1. The right one is regular and the left one is irregular. In order to review a few concepts, take the right T-mesh in Fig. 1 for example and the definitions of these concepts have been presented in [16,8].

- Vertices of a T-mesh: A grid point of a T-mesh is called a vertex of this T-mesh. In the right T-mesh of Fig. 1, $\{v_i\}_{i=1}^{15}$ are the vertices of the T-mesh and v_{11} is a crossing vertex. v_2, v_4, v_{12} , etc. are T-vertices. A vertex is called a boundary vertex if it lies on the boundary of the domain occupied by this T-mesh, otherwise, it is called an interior vertex. For example, $v_1, v_2, \dots, v_6, v_7, v_9, v_{10}, v_{15}$ are boundary ones and $v_8, v_{11}, v_{12}, v_{13}, v_{14}$ are interior ones.
- Edges of a T-mesh: A line segment connecting two adjacent vertices on a grid line is called an edge of a T-mesh; such line segments include v_1v_2 and v_2v_{11} , where v_1v_2 is a horizontal edge and v_2v_{11} is a vertical edge. v_1v_2, v_4v_5 , etc. are called boundary edges. $v_{12}v_{11}$ and v_2v_{11} are called interior edges.
- C-edges of a T-mesh: A composite edge (c-edge) [8] is a line segment that consists of several interior edges. It is the longest possible line segment, the inner vertices (all vertices except the end points of the line segment) of which are all T-vertices. $v_{10}v_{11}, v_5v_9$ are c-edges of the right T-mesh of Fig. 1. For the line segment $v_{10}v_{11}$, it cannot be extended since v_{11} is a crossing vertex and v_{11} is an inner vertex if we extend $v_{10}v_{11}$ to $v_{10}v_4$. Moreover, $v_{10}v_{11}$'s inner vertex is v_{13} and v_{13} is a T-vertex; For the segment v_5v_9 , it cannot be extended and its inner vertices $\{v_8, v_{12}, v_{14}\}$ are T-vertices. Thus, $v_{10}v_{11}, v_5v_9$ are c-edges of this T-mesh.
- Cells of a T-mesh: In the right T-mesh of Fig. 1, the region occupied by the rectangle $v_1v_2v_{11}v_{10}$ is a cell of this T-mesh. For this cell, the vertices v_1, v_2, v_{11}, v_{10} are called the corner vertices of this cell. The line segment $v_{10}v_{11}$ is called an edge of this cell, although $v_{10}v_{11}$ is not an edge of this T-mesh.

A *hierarchical T-mesh* is a special T-mesh defined in a recursive fashion. Initially a tensor product mesh (level 0) is presumed. Cells of this tensor product mesh are called cells at level 0. From level k to $k + 1$, some cells at level k are subdivided

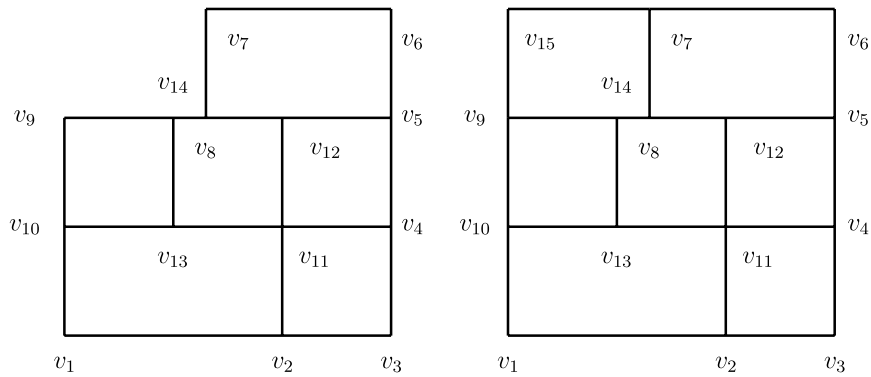


Fig. 1. Examples of T-meshes.

by connecting the middle points of the opposite edges with two straight lines. Four sub-cells are generated for each cell. These new cells are called cells at level $k + 1$. Fig. 2 illustrates a sequence of hierarchical T-meshes.

Specially, for any c-edge of a hierarchical T-mesh, it is an edge of a cell of this hierarchical T-mesh since each new c-edge generated at level $k + 1$ is an edge of a cell of this hierarchical T-meshes.

Given a T-mesh \mathcal{T} , \mathcal{F} is the set of all of the cells of \mathcal{T} and Ω is the region occupied by cells in \mathcal{F} . Spline spaces over T-meshes are defined by

$$\mathbf{S}(m, n, \alpha, \beta, \mathcal{T}) := \{f(x, y) \in C^{\alpha, \beta}(\Omega) : f(x, y)|_{\phi} \in \mathbb{P}_{m, n}, \forall \phi \in \mathcal{F}\}, \tag{1}$$

where $\mathbb{P}_{m, n}$ is the space of all of the polynomials of bi-degree (m, n) , and $C^{\alpha, \beta}(\Omega)$ is the space consisting of all of the bivariate functions that are continuous in Ω with order α along the x -direction and order β along the y -direction. Specially, if \mathcal{T} is a hierarchical T-mesh, $\mathbf{S}(3, 3, 1, 1, \mathcal{T})$ is called as a spline space of PHT (i.e., polynomial splines over hierarchical T-meshes) in [16]. Recently, this type of splines have been used to traditional FEM [18] and Isogeometric analysis [19,20] not only used in CAGD.

2.2. Splines with mixed orders of continuity over T-meshes

Based on the concepts presented in the previous section, spline spaces with mixed orders of continuity over T-meshes can be defined.

Definition 2.1. Let $E^v = \{e_i^v\}_{i=1}^s$ and $E^h = \{e_j^h\}_{j=1}^t$ be sets of vertical edges and horizontal edges of a T-mesh \mathcal{T} respectively. \mathcal{F} is the set of all of the cells of \mathcal{T} . A function $f(x, y)$ is defined over the region Ω occupied by all of the cells of \mathcal{T} . The function is a spline function with $C^{\{\alpha_i\}_{i=1}^s, \{\beta_j\}_{j=1}^t}$ if it satisfies the following conditions:

- $f(x, y)|_{\phi} \in \mathbb{P}_{m, n}$, where $\phi \in \mathcal{F}$ and $\mathbb{P}_{m, n}$ is the space of all of the polynomials of bi-degree (m, n) ;
- $f(x, y)$ is a function with continuity of order α_i at each point within e_i^v along the x -direction and with continuity of order β_j at each point within e_j^h along the y -direction, where $-1 \leq \alpha_i \leq m, -1 \leq \beta_j \leq n, i = 1, 2, \dots, s, j = 1, 2, \dots, t$;
- If e is a vertical (horizontal) boundary edge, then $\alpha_e = -1$ ($\beta_e = -1$), where α_e (or β_e) is the order of continuity along the direction that is perpendicular to e .

All spline functions satisfying these conditions compose a spline space with mixed orders of continuity over \mathcal{T} denoted by $\mathbf{S}(m, n, \{\alpha_i\}_{i=1}^s, \{\beta_j\}_{j=1}^t, \mathcal{T})$. By this definition, for a vertex v of \mathcal{T} , let $e_1^v, e_2^v, \dots, e_k^v$ be the edges with v as an endpoint and $\alpha_{e_1}, \dots, \alpha_{e_1}, \beta_{e_{k+1}}, \dots, \beta_{e_k}$ be their continuity orders respectively. Then, the continuity order at v is $\min\{\alpha_{e_1}, \dots, \alpha_{e_1}, \beta_{e_{k+1}}, \dots, \beta_{e_k}\}$.

In this paper, we will focus on spline spaces with $m = 3, n = 3$ and $\alpha_i, \beta_j \in \{1, -1\}$ over hierarchical T-meshes. We also call the spline function in this space combined PHT (C-PHT) named after PHT in [16]. If e_i^v (e_j^h) is of $\alpha_i = -1$ ($\beta_j = -1$), e_i^v (e_j^h) is called a discontinuous edge (D-edge for short).

The space of C-PHT is determined by the T-mesh \mathcal{T} associated with the continuity order of each edge. This type of \mathcal{T} , with continuity orders, is denoted \mathcal{T}_c , and the space of C-PHT determined by \mathcal{T}_c is denoted $\mathbf{S}(\mathcal{T}_c)$. For example, in Fig. 3, there is a T-mesh \mathcal{T}_c with the continuity orders, where the continuity orders of the edges in red are -1 and others are 1 . Thus, this information determines the C-PHT space defined over \mathcal{T}_c totally.

3. Dimension formulae of spaces of C-PHT

In this section, we present the dimensional formulae of C-PHT spline spaces. First, the B-net method of bicubic splines over T-meshes is reviewed which is a basic tool used in the proof of dimension formulas. Then, we introduce a few concepts to facilitate the expression of dimensional formulae and prove the dimensional formulae in the final part of this section.

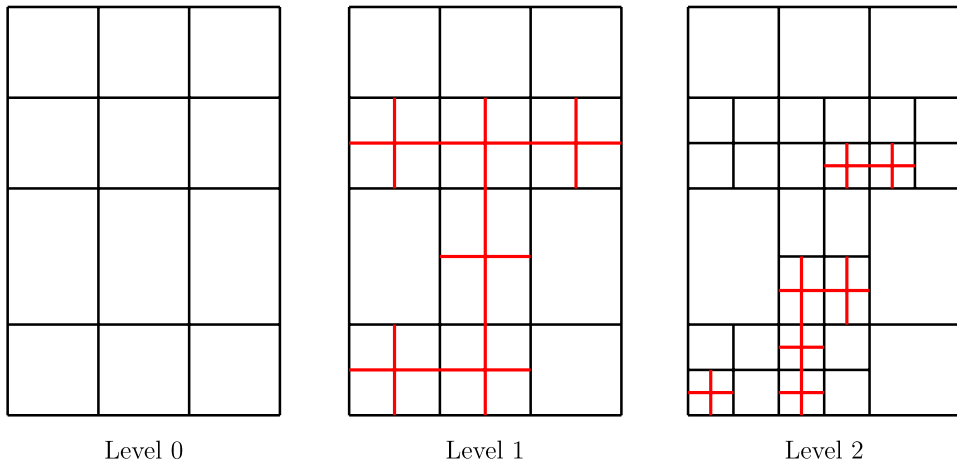


Fig. 2. Hierarchical T-meshes.

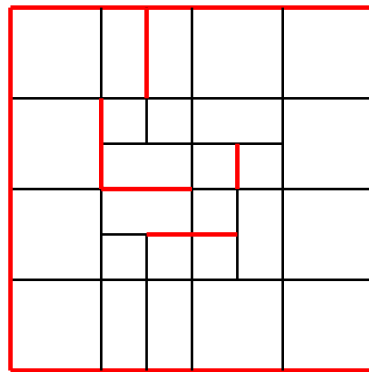


Fig. 3. A T-mesh \mathcal{T}_c with the continuity orders and its C-PHT space $\mathbf{S}(\mathcal{T}_c)$. (For interpretation of the references to colour in this figure legend, the reader is referred to the web version of this article.)

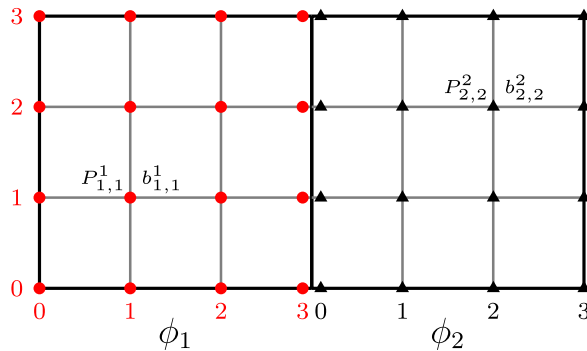


Fig. 4. The Bézier ordinates b_{ij}^k and P_{ij}^k of two bi-cubic polynomials.

3.1. The B-net method

In the theory of multi-variate splines, there are several approaches used to calculate the dimension of a spline space, such as the B-net method [5]. In this section, we review the B-net method for the case of bicubic splines over T-meshes.

Let $f_1(x, y)$ and $f_2(x, y)$ be two bicubic polynomials defined over two adjacent domains ϕ_1 and ϕ_2 respectively, shown in Fig. 4, where $\phi_1 = [x_0, x_1] \times [y_0, y_1]$ and $\phi_2 = [x_1, x_2] \times [y_0, y_1]$. There are $\{b_{ij}^1 \in \mathbb{R} : i, j = 0, 1, 2, 3\}$ such that

$$f_1(x, y) = \sum_{i,j=0}^3 b_{ij}^1 B_{ij}^1(x, y),$$

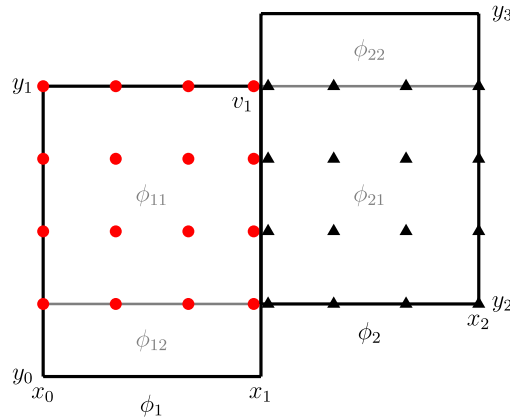


Fig. 5. The Bézier ordinates for two horizontal adjacent cells.

where

$$B_{i,j}^1(x, y) = N[\underbrace{x_0, \dots, x_0}_{4-i}, \underbrace{x_1, \dots, x_1}_{i+1}](x) \cdot N[\underbrace{y_0, \dots, y_0}_{4-j}, \underbrace{y_1, \dots, y_1}_{j+1}](y). \tag{2}$$

Here $N[t_0, t_1, \dots, t_s](t)$ is a B-spline function defined by the knots $t_0 \leq t_1 \leq \dots \leq t_s$. Similarly, $f_2(x, y)$ can be expressed by $\{B_{i,j}^2(x, y)\}$ with coefficients $\{b_{i,j}^2\}$, where $B_{i,j}^2(x, y)$ is defined similarly to $B_{i,j}^1(x, y)$ by Eq. (2). $\{b_{i,j}^1\}$ and $\{b_{i,j}^2\}$ are called the Bézier ordinates of $f_1(x, y)$ and $f_2(x, y)$, respectively. It is well known that $f_1(x, y)$ and $f_2(x, y)$ are r -time differentiable across their common boundary if and only if [5]

$$\frac{1}{(x_1 - x_0)^i} \Delta^{i,0} b_{3-i,j}^1 = \frac{1}{(x_2 - x_1)^i} \Delta^{i,0} b_{0,j}^2, \tag{3}$$

where $j = 0, 1, 2, 3, i = 0, 1, \dots, r, \Delta^{i,0} b_{j,k} = \Delta^{i-1,0} b_{j+1,k} - \Delta^{i-1,0} b_{j,k}$ with $\Delta^{0,0} b_{j,k} = b_{j,k}$. In particular, when $f_1(x, y)$ and $f_2(x, y)$ are one-time differentiable across their common boundary, i.e., $r = 1$, by Eq. (3), $\{b_{i,j}^1\}_{i,j=0}^3$ and $\{b_{i,j}^2\}_{i,j=0}^3$ satisfy

$$\begin{aligned} b_{3,j}^1 &= b_{0,j}^2, \\ b_{2,j}^1 &= \left(1 + \frac{x_1 - x_0}{x_2 - x_1}\right) b_{0,j}^2 - \frac{x_1 - x_0}{x_2 - x_1} b_{1,j}^2, \end{aligned} \tag{4}$$

where $j = 0, 1, 2, 3$.

Let $\mathcal{B}(\phi_1) = \{P_{i,j}^1\}_{i,j=0}^3$ and $\mathcal{B}(\phi_2) = \{P_{i,j}^2\}_{i,j=0}^3$ be point sets in the cells ϕ_1 and ϕ_2 , where the coordinates of $P_{i,j}^1$ as $\left(\frac{(3-i)x_0 + ix_1}{3}, \frac{(3-j)y_0 + jy_1}{3}\right)$ and $P_{i,j}^2$ as $\left(\frac{(3-i)x_1 + ix_2}{3}, \frac{(3-j)y_0 + jy_1}{3}\right)$. For example, in Fig. 4, the circular point set is $\mathcal{B}(\phi_1)$ and the triangular point set is $\mathcal{B}(\phi_2)$.

We can construct a bijection τ between $\{P_{i,j}^1\}_{i,j=0}^3$ and $\{P_{i,j}^2\}_{i,j=0}^3$ by $\tau(P_{i,j}^1) = P_{i,j}^2$, $i, j = 0, 1, 2, 3$. By this correspondence, $b_{i,j}^1$ can be treated as the Bézier ordinate of $P_{i,j}^1$ associated with $f_1(x, y)$.

Thus, $f_1(x, y)$ and $f_2(x, y)$ with continuity of order 1 (Eq. (4)) can be expressed by the sets $\mathcal{B}(\phi_1)$ and $\mathcal{B}(\phi_2)$ by using τ .

When T-meshes are considered, we must discuss two adjacent cells in a general position. In the following, this case will be summed up in the former one by splitting cells. For two general horizontal adjacent cells $\phi_1 = [x_0, x_1] \times [y_0, y_1]$ and $\phi_2 = [x_1, x_2] \times [y_2, y_3]$ (Fig. 5), the continuous conditions expressed by Bézier ordinates are defined by the domains $[x_0, x_1] \times [\bar{y}_0, \bar{y}_1]$ and $[x_1, x_2] \times [\bar{y}_0, \bar{y}_1]$, where $\bar{y}_0 = \max\{y_0, y_2\}$ and $\bar{y}_1 = \min\{y_1, y_3\}$. The Bézier ordinates in ϕ_1 (or ϕ_2) can be completely determined by the Bézier ordinates in $[x_0, x_1] \times [\bar{y}_0, \bar{y}_1]$ (or $[x_1, x_2] \times [\bar{y}_0, \bar{y}_1]$) because there is only one polynomial over ϕ_1 (or ϕ_2). To be more specific, we suppose that ϕ_1 is split into ϕ_{11} and ϕ_{12} in Fig. 5. The Bézier ordinates of $\mathcal{B}(\phi_{11})$ determine the Bézier ordinates of $\mathcal{B}(\phi_{12})$ as having continuity of order 3 along the common edge according to Eq. (3). Thus, the Bézier ordinates of $\mathcal{B}(\phi_1)$ are obtained. Similar continuity conditions can be derived for any two vertical adjacent cells.

Let \mathcal{T} be a T-mesh, and $\mathcal{F} = \{\phi_1, \phi_2, \dots, \phi_l\}$ is a set of all its cells, where $\phi_k = [x_0^k, x_1^k] \times [y_0^k, y_1^k]$. Define the point set

$$\mathcal{B}(\mathcal{F}) = \cup_{k=1}^l \mathcal{B}(\phi_k),$$

where $\mathcal{B}(\phi_k) = \{P_{i,j}^k\}_{i,j=0}^3$.

For $f(x, y) \in \mathbf{S}(\mathcal{F})$, $f(x, y)|_{\phi_k} \in \mathbb{P}_{3,3}$. Therefore, a linear functional $\lambda_{P_{i,j}^k}$ can be defined for each $P_{i,j}^k \in \mathcal{B}(\phi_k)$ by

$$\lambda_{P_{i,j}^k}(f(x, y)) = b_{i,j}^k,$$

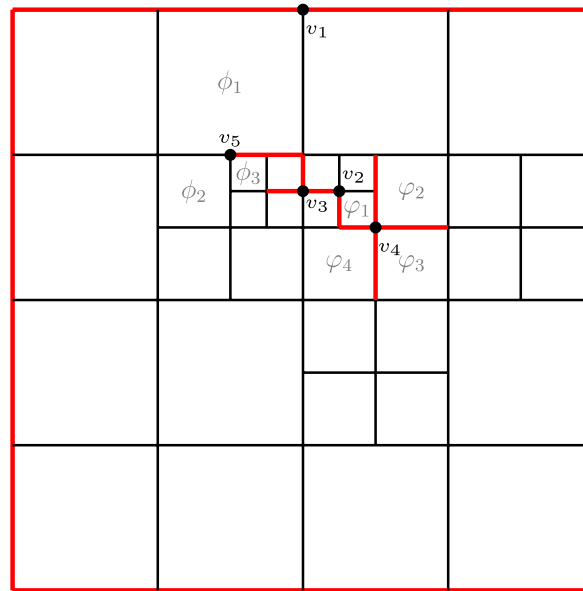


Fig. 6. The undirected graph G of a space of discontinuous PHT. (For interpretation of the references to colour in this figure legend, the reader is referred to the web version of this article.)

where $b_{i,j}^k$ is the Bézier ordinate of $f(x, y)|_{\phi_k}$ associated with $P_{i,j}^k$. A set of points $\mathcal{P} \subset \mathcal{B}(\mathcal{T})$ is called a *determining set* [21] for the spline space $\mathbf{S}(\mathcal{T}_C)$, if $\lambda_P(f(x, y)) = 0 (\forall P \in \mathcal{P})$ indicates that $f(x, y) = 0$, for any $f(x, y) \in \mathbf{S}(\mathcal{T}_C)$. If \mathcal{P} is a determining set of $\mathbf{S}(\mathcal{T}_C)$, then

$$\dim \mathbf{S}(\mathcal{T}_C) \leq \#\mathcal{P}.$$

If each nontrivial subset of \mathcal{P} is not a determining set of $\mathbf{S}(\mathcal{T}_C)$, then \mathcal{P} is called a *minimal determining set* and

$$\dim \mathbf{S}(\mathcal{T}_C) = \#\mathcal{P},$$

where $\#\mathcal{P}$ is the cardinality of \mathcal{P} . The dimensional formulae of $\mathbf{S}(\mathcal{T}_C)$ will be derived using this method in the following section. To describe a minimal determining set of $\mathbf{S}(\mathcal{T}_C)$, a few concepts of point sets are presented at first.

3.2. Some concepts

Let \mathcal{T} be a hierarchical T-mesh. $E^v = \{e_i^v\}_{i=1}^s$ and $E^h = \{e_j^h\}_{j=1}^t$ are the sets of vertical edges and horizontal edges of \mathcal{T} respectively. $\phi_k, \mathcal{B}(\phi_k)$ and $\mathcal{B}(\mathcal{T})$ are defined as before, where $k = 1, 2, \dots, l$.

The graph $G_D = (V_D, E_D)$ is defined by \mathcal{T}_C in the following fashion. Here,

$$E_D := \{e : e \text{ is a D-edge of } \mathcal{T}_C\},$$

and the vertex set V_D consists of all of the vertices of \mathcal{T} on the edges in E_D . Let

$$\mathcal{F}_v = \{C \in \mathcal{T} : v \text{ is on the boundary of } C\}$$

be the set of cells that are related to a vertex $v \in V_{\mathcal{T}}$, where $V_{\mathcal{T}}$ is the set of vertices of \mathcal{T} . Then G_D can be used to classify these cells. Specifically, the domain occupied by all of the cells in \mathcal{F}_v can be divided into several connected components by G_D . Each connected component consists of some cells in \mathcal{F}_v , and

$$\mathcal{F}_v = \Omega_1 \cup \Omega_2 \cup \dots \cup \Omega_r,$$

where Ω_i is the cell set formed the *ith connected component* and $\Omega_i \cap \Omega_j = \emptyset (i \neq j), i, j = 1, 2, \dots, r$.

By this classification, in Fig. 6, $\mathcal{F}_{v_5} = \{\phi_1, \phi_2, \phi_3\}$ and $\mathcal{F}_{v_4} = \{\phi_1, \phi_2, \phi_3, \phi_4\}$. For the vertex $v \notin V_D$, there is only one connected component of \mathcal{F}_v . The numbers of connected components of v_5 and v_4 are 1 and 4 respectively.

Generally, for $v \in V_{\mathcal{T}}$, the number of connected components equals to $\deg v$, where $\deg v = 0$, if $v \notin V_D$; otherwise, $\deg v$ is the degree of v in the sense of the graph G_D .

For a cell ϕ and its point set $\mathcal{B}(\phi)$, $\mathcal{B}(\phi)$ can be divided into 4 disjoint sets associated with 4 corner vertices of ϕ . If Q is one of the corner vertices of ϕ , the subset of $\mathcal{B}(\phi)$ associated with Q consists of the nearest 4 points of Q in $\mathcal{B}(\phi)$, denoted as $\mathcal{B}_{Q,\phi}$. This procedure is illustrated in Fig. 7. Points in different subsets are distinguished from each other with different shapes.

For each vertex v of \mathcal{T} , the point set \mathcal{P}_Ω^v is defined as follows.

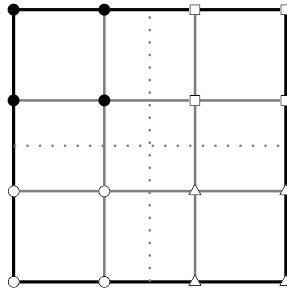


Fig. 7. The subsets of $\mathcal{B}(\phi)$.

Definition 3.1. Ω is a connected component of v , where v is a vertex of \mathcal{T} . If there is a cell $\phi \in \Omega$ of \mathcal{T} and v is not a corner vertex of ϕ , $\mathcal{P}_\Omega^v = \emptyset$. Otherwise, there is a cell ϕ of \mathcal{T} such that v is a corner vertex of ϕ . Then $\mathcal{P}_\Omega^v = \mathcal{B}_{v,\phi}$.

The following should be noted regarding this definition. If there is another cell φ satisfying conditions besides ϕ , the Bézier ordinates of $\mathcal{B}_{v,\varphi}$ and $\mathcal{B}_{v,\phi}$ are equivalent from a “determining set” point of view according to Eq. (4). Thus, the definition of \mathcal{P}_Ω^v is independent of the choice of ϕ from the view of a determining set. Specifically, the Bézier ordinates of $\mathcal{B}_{v,\phi}$ are zeros if and only if the Bézier ordinates of $\mathcal{B}_{v,\varphi}$ are zeros. This result will be used in the proof of dimensional formulae in Section 3.3.

Let $\{\Omega_1, \Omega_2, \dots, \Omega_r\}$ be all of the connected components of v , where $\mathcal{P}^v = \cup_{i=1}^r \mathcal{P}_{\Omega_i}^v$ is called the set of points associated with v .

In Fig. 6, there are four connected components of v_4 and $\mathcal{P}^{v_4} = \cup_{i=1}^4 \mathcal{P}_{\phi_i}^{v_4}$, where $\mathcal{P}_{\phi_i}^{v_4} = \mathcal{B}_{v_4,\phi_i}$. In addition, $\mathcal{P}^{v_5} = \emptyset$ because there is a cell ϕ_1 in the unique connected component of v_5 , and v_5 is not a corner vertex of ϕ_1 .

3.3. Dimensional formulae

Based on the concepts defined in the previous section, the dimensional formulae of a space of C-PHT is presented by the following theorem.

Theorem 3.1. Let $\mathbf{S}(\mathcal{T}_C)$ be a space of C-PHT over a hierarchical T-mesh \mathcal{T} , where \mathcal{T}_C is \mathcal{T} associated with continuity orders. $G_D = (V_D, E_D)$ is the graph defined by \mathcal{T}_C . Thus,

$$\dim \mathbf{S}(\mathcal{T}_C) = 4V^+ + \sum_{v \in V_D} 4(\deg v - 1),$$

where V^+ is the number of crossing vertices of \mathcal{T} and $\deg v$ is the degree of v in G_D .

Proof. Let $V_{\mathcal{T}}$ be the set of vertices of \mathcal{T} . Denote $\mathcal{P} = \cup_{v \in V_{\mathcal{T}}} \mathcal{P}^v$, where \mathcal{P}^v is the set of points associated with v . We will demonstrate that \mathcal{P} is a determining set of $\mathbf{S}(\mathcal{T}_C)$.

For a spline function $f(x, y) \in \mathbf{S}(\mathcal{T}_C)$, the function satisfies $\lambda_P(f(x, y)) = 0$ for all $P \in \mathcal{P}$. For any $P_{i,j}^k \in \mathcal{B}(\mathcal{T}) \setminus \mathcal{P}$, there is a unique cell ϕ_k and a unique vertex $v_0 \in V_{\mathcal{T}}$ such that $P_{i,j}^k \in \mathcal{B}_{v_0,\phi_k}$. Let Ω be the connected component of v_0 and $\phi_k \in \Omega$. Thus $\mathcal{P}_\Omega^{v_0} \subset \mathcal{P}^{v_0}$. We first consider two cases.

- a. v_0 is a crossing vertex of \mathcal{T} . Thus, v_0 is one of corner vertices of these cells around v_0 . According to the definition of $\mathcal{P}_\Omega^{v_0}$, $\mathcal{P}_\Omega^{v_0} \neq \emptyset$. Therefore, the Bézier ordinates of \mathcal{B}_{v_0,ϕ_k} are zeros because the ordinates of $\mathcal{P}_\Omega^{v_0}$ are zeros. Specifically, $\lambda_{P_{i,j}^k}(f(x, y)) = 0$.
- b. v_0 is a T-vertex of \mathcal{T} . If $\mathcal{P}_\Omega^{v_0} \neq \emptyset$, $\lambda_{P_{i,j}^k}(f(x, y)) = 0$ can be obtained by using the same method as described above.

In the following, we will consider the case $\mathcal{P}_\Omega^{v_0} = \emptyset$ for a T-vertex v_0 . Let $v_{01}v_{02}$ be the c-edge with endpoints v_{01} and v_{02} such that v_0 is one of its inner vertices. Thus, there is a cell ϕ_1 with $v_{01}v_{02}$ as one of its edges because \mathcal{T} is a hierarchical T-mesh. ϕ_k and ϕ_1 are in the same connected component of v_0 because $\mathcal{P}_\Omega^{v_0} = \emptyset$. Thus, the Bézier ordinates of \mathcal{B}_{v_0,ϕ_k} are determined by the Bézier ordinates of $\mathcal{B}_{v_{01},\phi_1} \cup \mathcal{B}_{v_{02},\phi_1}$. If the Bézier ordinates of $\mathcal{B}_{v_{01},\phi_1}$ (or $\mathcal{B}_{v_{02},\phi_1}$) can be determined to be zeros by $\mathcal{P}^{v_{01}}$ (or $\mathcal{P}^{v_{02}}$), then the progress is terminated. Else treat v_{01} (or v_{02}) as v_0 and repeat this progress. Here, this progress can be described as a binary tree structure shown in Fig. 8. According to the structure of a hierarchical T-mesh, the vertices that appear in the process are different from each other, and this process must be terminated after several steps. The leaf nodes of this binary tree are the point sets whose Bézier ordinates are zeros, since they are determined by the Bézier ordinates of \mathcal{P} for $f(x, y)$. Thus, the Bézier ordinates of \mathcal{B}_{v_0,ϕ_k} are zeros. Specifically, $\lambda_{P_{i,j}^k}(f(x, y)) = 0$.

Thus, according to the discussion above, \mathcal{P} is a determining set of $\mathbf{S}(\mathcal{T}_C)$. Moreover, if any point Q is removed from \mathcal{P} , a non-zero spline function $g(x, y) \in \mathbf{S}(\mathcal{T}_C)$ can be constructed with $\lambda_Q(g(x, y)) = 1$ and $\lambda_P(g(x, y)) = 0$, for all $P \in \mathcal{P} \setminus \{Q\}$. Thus \mathcal{P} is a minimal determining set of $\mathbf{S}(\mathcal{T}_C)$.

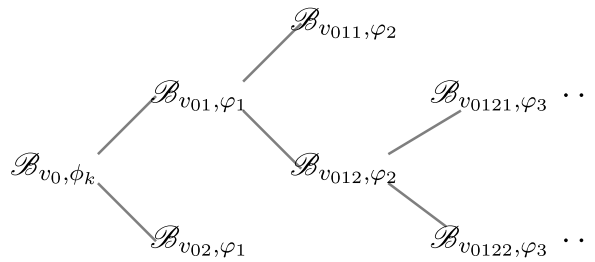


Fig. 8. The tree of relationships among Bézier ordinate sets.

For $v \in V_{\mathcal{T}} \setminus V_D$,

$$\#\mathcal{P}^v = \begin{cases} 4, & v \text{ is a crossing vertex;} \\ 0, & v \text{ is a T-vertex.} \end{cases}$$

For $v \in V_D$, the number of connected components of v is $\deg v$, therefore,

$$\#\mathcal{P}^v = \begin{cases} 4 \deg v, & v \text{ is a crossing vertex;} \\ 4(\deg v - 1), & v \text{ is a T-vertex.} \end{cases}$$

Thus,

$$\dim \mathbf{S}(\mathcal{T}_C) = 4V^+ + \sum_{v \in V_D} 4(\deg v - 1),$$

where V^+ is the number of crossing vertices of \mathcal{T} and $\deg v$ is the degree of v in G . \square

4. Basis functions of spaces of C-PHT

In practice, it is important to construct a set of basis functions with suitable properties. In this section, an algorithm for generating a hierarchical T-mesh with D-edges are given at first. Then, based on this algorithm, a set of bases with local support, non-negativity and partition of unity is presented.

4.1. Generation of a hierarchical T-mesh with D-edges

There are two types of operations that can be used to change the structure of a hierarchical T-mesh \mathcal{T} with D-edges denoted as \mathcal{T}_C . One is setting D-edges, the other is subdividing cells of \mathcal{T} . Here is an algorithm for generating a class of hierarchical T-mesh with D-edges.

Let $E_{\mathcal{T}_C}$ be the set of interior edges of \mathcal{T}_C . $C_{\mathcal{T}_C}^{TL}$ is a set of its cells at the top level. $\mathcal{B}(\mathcal{T}_C)$ is a set of basis functions of the space of C-PHT over \mathcal{T}_C and it should satisfy the given conditions denoted by \mathcal{C} eventually. \mathcal{T}_{\otimes} is an initial tensor product mesh.

Set all boundary edges of \mathcal{T}_{\otimes} as D-edges and denote the current T-mesh with continuity orders as \mathcal{T}'_{\otimes}

$\mathcal{T}_C \leftarrow \mathcal{T}'_{\otimes}$

Choose a set $\mathcal{E} \subset E_{\mathcal{T}_C}$

while $\mathcal{B}(\mathcal{T}_C)$ does not satisfy \mathcal{C} **do**

 Set all of the edges in \mathcal{E} as D-edges and denote the current T-mesh \mathcal{T}'_C

$\mathcal{T}_C \leftarrow \mathcal{T}'_C$

if $\mathcal{B}(\mathcal{T}_C)$ does not satisfy \mathcal{C} **then**

 Choose a set $\mathcal{C} \subset C_{\mathcal{T}_C}^{TL}$ and subdivide all of the cells in \mathcal{C} . Denote the current T-mesh \mathcal{T}'_C .

$\mathcal{E} \leftarrow$ A subset of $E_{\mathcal{T}'_C}$ and any edge in this subset with an endpoint at the center point of a cell in \mathcal{C}

$\mathcal{T}_C \leftarrow \mathcal{T}'_C$

end if

end while

In the following, there is an example shown in Fig. 9 that illustrates a sequence of a hierarchical T-mesh by this algorithm and this type of hierarchical T-mesh with D-edges is called a *hierarchical T-mesh with incomplete D-edges*.

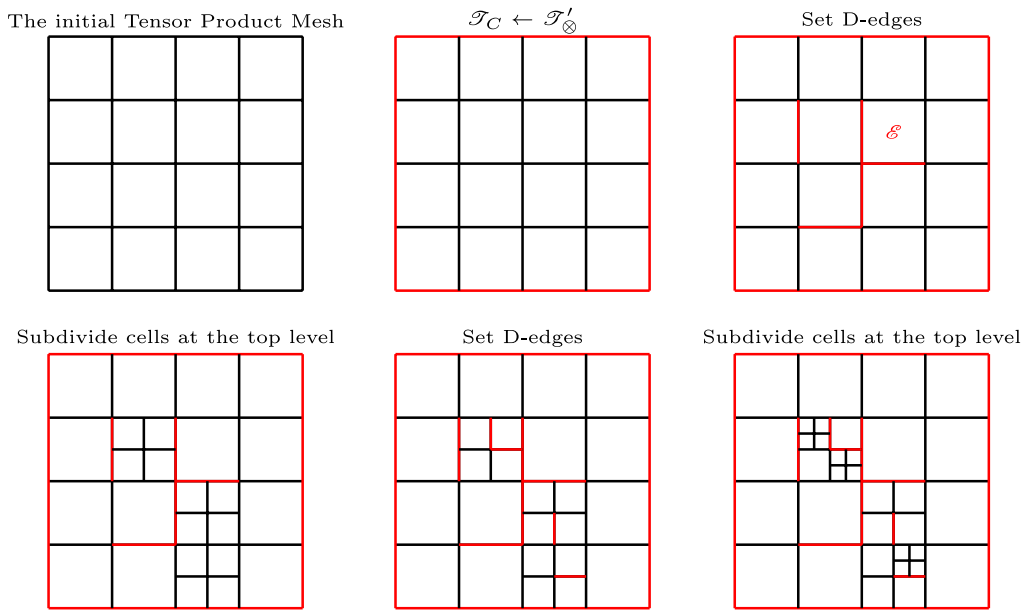


Fig. 9. A generation progress of a hierarchical T-mesh with D-edges by the algorithm in Section 4.1, where the continuity orders of the edges in red are –1 and others are 1. (For interpretation of the references to colour in this figure legend, the reader is referred to the web version of this article.)

4.2. Construction of basis functions

In this section, a set of basis functions of a space of C-PHT defined over a hierarchical T-mesh with incomplete D-edges is constructed with nonnegativity, local support and partition of unity. This construction process is recursive in generating \mathcal{T}_C defined in Section 4.1.

The basis functions of $\mathbf{S}(3, 3, 1, 1, \mathcal{T}'_{\otimes})$, where \mathcal{T}'_{\otimes} is the initial tensor product T-mesh, are standard tensor product B-splines. These functions are with non-negativity, local support and partition of unity naturally. Now, suppose there is a set of basis functions \mathcal{B}_0 with these properties before setting D-edges in \mathcal{E} . When an edge in \mathcal{E} is set as a D-edge, the set of basis functions \mathcal{B}_1 consists of two parts. The first part is composed of new basis functions associated with this edge which we prepare to set as a D-edge. The second part is composed of functions formed by modifying the functions in \mathcal{B}_0 .

1. New basis functions: Based on Theorem 3.1, when an edge v_1v_2 is set as a D-edge, new basis functions corresponding to the points that are added to \mathcal{P}^{v_1} and \mathcal{P}^{v_2} can be constructed, where v_1, v_2 are endpoints of the edge v_1v_2 . These endpoints are classified into crossing vertices and T-vertices.

(a) v is a crossing vertex. All of the cases are collected in Table 1, where,

$$N_1(s) = N[s_1, s_1, s_1, s_1, s_2](s), \quad N_2(s) = N[s_1, s_1, s_1, s_2, s_2](s),$$

$$N_3(t) = N[t_1, t_1, t_1, t_1, t_2](t), \quad N_4(t) = N[t_1, t_1, t_1, t_2, t_2](t),$$

$$N_5(t) = N[t_0, t_0, t_1, t_1, t_2](t), \quad N_6(t) = N[t_0, t_1, t_1, t_2, t_2](t)$$

and $N[x_1, x_2, x_3, x_4, x_5](x)$ is a cubic B-spline function defined by the knots $x_1 \leq x_2 \leq x_3 \leq x_4 \leq x_5$.

(b) v is a T-vertex. All of the cases are collected in Table 2, where $\{N_i(t)\}_{i=3}^6$ are the same as case (a) and $N_1(s) = N[s_0, s_0, s_0, s_0, s_1](s), N_2(s) = N[s_0, s_0, s_0, s_1, s_1](s)$.

2. Modification of the old basis functions: The function $f(x, y) \in \mathcal{B}_0$ is represented by Bézier ordinates on each cell. $f(x, y)$ is modified by setting all of the Bézier ordinates of the points in the point sets shown in Tables 1 and 2 as zeros.

It is easy to verify that the functions in \mathcal{B}_1 possess the properties of local support and non-negativity. The partition of unity of \mathcal{B}_1 will be verified in the following.

Let $\mathcal{B}_0 = \{f_i(x, y)\}$ with $\sum_i f_i(x, y) \equiv 1$ and $\{g_j(x, y)\}$ be the new basis functions that are added to the first part. Thus, all the Bézier ordinates of $\sum_i f_i(x, y)$ are ones, and the Bézier ordinates of $\sum_j g_j(x, y)$ associated with the points in the point sets are ones. By modifying in the second part, all of the Bézier ordinates of the sum of all of the functions in \mathcal{B}_1 are ones, i.e., \mathcal{B}_1 has the partition of unity.

Thus, suppose there is a set of basis functions \mathcal{B}_1 with the properties of local support, non-negativity and partition of unity before subdividing the cells in \mathcal{C} . Let \mathcal{B}_2 be the set of basis functions constructed after subdividing one of the cells in \mathcal{C} . \mathcal{B}_2 consists of two disjoint parts. One is the set of new functions added; the other is the set of functions generated by modifying the functions in \mathcal{B}_1 .

Table 1

The collection of all cases when v is a crossing vertex, where the knots of the tensor product mesh are $[s_0, s_1, s_2] \otimes [t_0, t_1, t_2]$ and the original D-edges are indicated by black solid lines and new D-edges by black broken lines. The upper left cell is labeled as ϕ_1 , and all other cells are labeled in counterclockwise fashion.

Cases	B-splines	Point sets
	\emptyset	\emptyset
	$\Delta_1 = \{N_1(s)N_3(t), N_1(s)N_4(t), N_2(s)N_3(t), N_2(s)N_4(t)\}$	\mathcal{B}_{v,ϕ_4}
	$\Delta_2 = \{N_1(s)N_5(t), N_1(s)N_6(t), N_2(s)N_5(t), N_2(s)N_6(t)\}$	$\mathcal{B}_{v,\phi_3} \cup \mathcal{B}_{v,\phi_4}$
	$\Delta_1 = \{N_1(s)N_3(t), N_1(s)N_4(t), N_2(s)N_3(t), N_2(s)N_4(t)\}$	\mathcal{B}_{v,ϕ_4}
	$\Delta_1 = \{N_1(s)N_3(t), N_1(s)N_4(t), N_2(s)N_3(t), N_2(s)N_4(t)\}$	\mathcal{B}_{v,ϕ_4}
	$\Delta_1 = \{N_1(s)N_3(t), N_1(s)N_4(t), N_2(s)N_3(t), N_2(s)N_4(t)\}$	\mathcal{B}_{v,ϕ_4}

Table 2

The collection of all of the cases when v is a T-vertex, where the knots of the tensor product mesh are $[s_0, s_1, s_2] \otimes [t_0, t_1, t_2]$, and the original D-edges are indicated by black solid lines and new D-edges by black broken lines. The upper left cell is labeled as ϕ_1 and all other cells are labeled in label others along the counterclockwise fashion.

Cases	B-splines	Point sets
	\emptyset	\emptyset
	\emptyset	\emptyset
	$\Delta_1 = \{N_1(s)N_3(t), N_1(s)N_4(t), N_2(s)N_3(t), N_2(s)N_4(t)\}$	\mathcal{B}_{v,ϕ_1}
	$\Delta_2 = \{N_1(s)N_5(t), N_1(s)N_6(t), N_2(s)N_5(t), N_2(s)N_6(t)\}$	$\mathcal{B}_{v,\phi_1} \cup \mathcal{B}_{v,\phi_2}$
	$\Delta_1 = \{N_1(s)N_3(t), N_1(s)N_4(t), N_2(s)N_3(t), N_2(s)N_4(t)\}$	\mathcal{B}_{v,ϕ_1}
	$\Delta_1 = \{N_1(s)N_3(t), N_1(s)N_4(t), N_2(s)N_3(t), N_2(s)N_4(t)\}$	\mathcal{B}_{v,ϕ_1}
	$\Delta_1 = \{N_1(s)N_3(t), N_1(s)N_4(t), N_2(s)N_3(t), N_2(s)N_4(t)\}$	\mathcal{B}_{v,ϕ_1}

1. New basis functions: When we subdivide a cell in \mathcal{C} , the new basis functions corresponding to the points that are added to \mathcal{P}^{v_1} and \mathcal{P}^{v_2} can be constructed, where v_1v_2 is a new edge and v_1, v_2 are endpoints of the edge v_1v_2 according to Theorem 3.1. Let v be an endpoint of a new edge by subdividing of a cell C in \mathcal{C} .

(a) v is the center point of the cell C . The new basis functions are

$$N_1(s) = N[s_0, s_0, s_1, s_1, s_2](s), \quad N_2(s) = N[s_0, s_1, s_1, s_2, s_2](s),$$

$$N_3(t) = N[t_0, t_0, t_1, t_1, t_2](t), \quad N_4(t) = N[t_0, t_1, t_1, t_2, t_2](t).$$

The new points associated with these functions are shown in Table 3.

(b) v is a crossing vertex of \mathcal{T}'_C and is not a center point of any cell in \mathcal{C} . There are 4 new basis functions based on the dimensional formula we proved. In Table 4, all cases of v are classified, and the new basis functions are presented.

(c) v is a T-vertex of \mathcal{T}'_C . Based on the dimensional formula, all cases of v and the new basis functions are collected in Table 5.

2. Modification of the old basis functions: The function $f(x, y) \in \mathcal{B}_1$ is represented by Bézier ordinates on each cell. $f(x, y)$ is modified by setting all of the Bézier ordinates of the points in point sets in Tables 3–5 as zeros.

The functions in \mathcal{B}_2 have the properties of local support, non-negativity and partition of unity. These facts can be verified in a manner similar to described above.

Table 3

The collection of all cases in which v is the center point of C , where the knots of the tensor product mesh are $[s_0, s_1, s_2] \otimes [t_0, t_1, t_2]$ and new edges with the center point C as an endpoint are indicated in black. The upper left cell is labeled as ϕ_1 and all other cells are labeled in counterclockwise fashion.

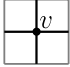
Cases	B-splines	Point sets
	$\Delta_1 = \{N_1(s)N_3(t), N_1(s)N_4(t), N_2(s)N_3(t), N_2(s)N_4(t)\}$	$\mathcal{B}_{v,\phi_1} \cup \mathcal{B}_{v,\phi_2} \cup \mathcal{B}_{v,\phi_3} \cup \mathcal{B}_{v,\phi_4}$

Table 4

The collection of all cases in which v is a crossing vertex of \mathcal{S}'_C and is not a center point of any cell in \mathcal{C} . The knots of the tensor product mesh are $[s_0, s_1, s_2] \otimes [t_0, t_1, t_2]$. Δ_1 is the same as Δ_1 in Table 3, and new edges with the center point C as an endpoint are indicated in black. The upper left cell is labeled as ϕ_1 , and all other cells are labeled in counterclockwise fashion.

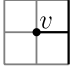
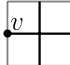
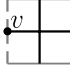
Cases	B-splines	Point sets
	$\Delta_1 = \{N_1(s)N_3(t), N_1(s)N_4(t), N_2(s)N_3(t), N_2(s)N_4(t)\}$	$\mathcal{B}_{v,\phi_1} \cup \mathcal{B}_{v,\phi_2} \cup \mathcal{B}_{v,\phi_3} \cup \mathcal{B}_{v,\phi_4}$

Table 5

The collection of all cases in which v is a T-vertex of \mathcal{S}'_C , where Δ_2 is the same as Δ_2 in Table 2 and new edges with the center point C as an endpoint are indicated in black. The original D-edges are indicated by broken gray lines. The knots of the tensor product mesh are $[s_0, s_1, s_2] \otimes [t_0, t_1, t_2]$. The upper left cell is labeled as ϕ_1 , and all other cells are labeled in counterclockwise fashion.

Cases	B-splines	Point sets
	\emptyset	\emptyset
	$\Delta_2 = \{N_1(s)N_5(t), N_1(s)N_6(t), N_2(s)N_5(t), N_2(s)N_6(t)\}$	$\mathcal{B}_{v,\phi_1} \cup \mathcal{B}_{v,\phi_2}$

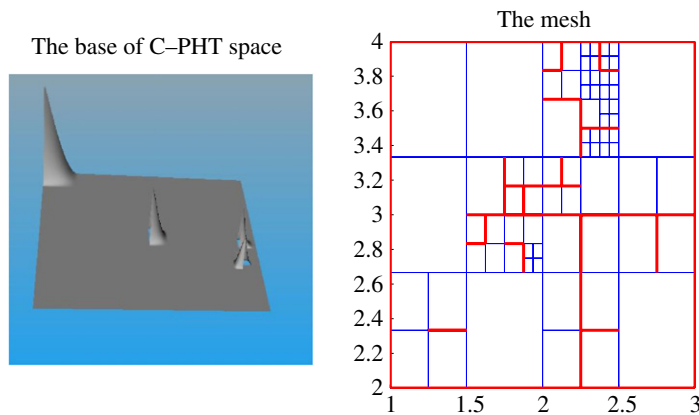


Fig. 10. An example of basis functions in a space of C-PHT.

In Fig. 10, some basis functions in a space of C-PHT are presented. The left image shows basis functions, and the right one shows the hierarchical T-mesh with incompleted D-edges of this C-PHT space.

5. Examples

In this section, C-PHT splines are applied to handle image data processing and solve a PDE that has a discontinuous solution.

5.1. Example 1: image data processing

C-PHT splines are a kind of splines which are used to keep the discontinuous characteristic of data. In this section, in order to seek a better visual effect, we choose image data in the left side of Fig. 11 as an experiment. The discontinuous

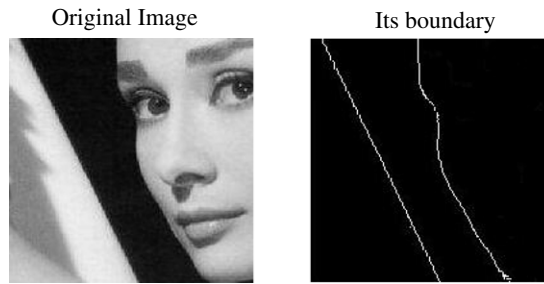


Fig. 11. An original image and its considered boundary.

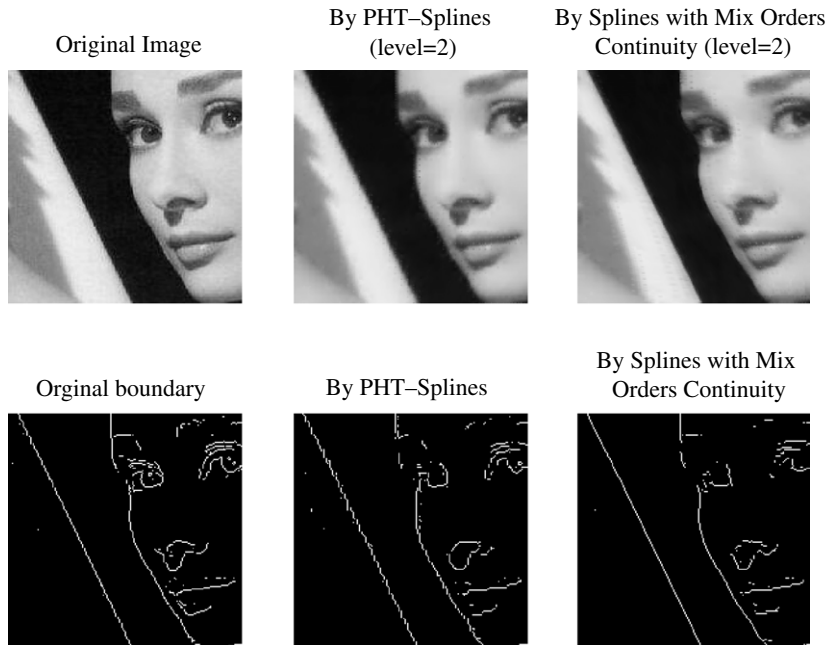


Fig. 12. Comparing fitting results of PHT and C-PHT.

part shown in the right side of Fig. 11 is the boundary which separates the object in this image from its background. Moreover, considering the structure of T-meshes, their reparameterization must be appreciated. Here we adopt the boundary parameterization method described in [22].

In Fig. 12, PHT-splines and C-PHT splines have been used to reconstruct the image. Under the same conditions, the boundary of these reconstructed images are obtained by the edge detection with the help of Matlab. From these detection results, the boundary of the image has noise by using PHT-splines. However, the boundary is maintained better by using C-PHT splines. Moreover, in Fig. 13, this discontinuous characteristic is kept, even though the image reconstructed by C-PHT splines is enlarged.

5.2. Example 2: solving PDE

Many physical problems can be described mathematically as PDEs. The finite element method (FEM) is commonly used to solve PDE. The choice of finite element space is important because a solution given by the FEM is a type of projection of a (weak) PDE solution in this finite element space. In other words, if a PDE has a discontinuous solution and we choose a smooth finite element space, the solution given by the FEM is smooth. If we want to obtain a discontinuous solution, we should choose a discontinuous finite element space such as a C-PHT space. Here, we consider a two-dimensional elliptic boundary value problem (BVP). As is known, the continuity of weak solutions of BVPs is affected by many factors, such as the shape of the physical domain of BVPs, the continuity of the coefficients and the function on the right-hand side of the corresponding elliptic equations.

Here we have two sub-examples for solving PDEs. The constrain of the first example is only on the boundary of the physical domain; The constrain of the second example is on the boundary and the D-edges.

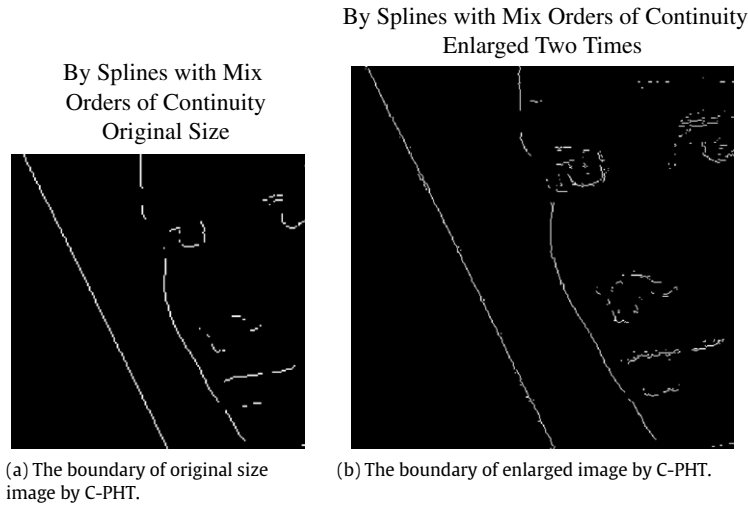


Fig. 13. Enlarge the image by C-PHT splines.

5.2.1. Example 2.1

The strong form of this BVP is as follows. Find $u : \overline{\Omega} \rightarrow \mathbb{R}$ such that

$$\begin{aligned} -\Delta u &= f \quad \text{in } \Omega, \\ u &= 0 \quad \text{on } \partial\Omega, \end{aligned}$$

where Ω is a rectangular domain $(0, 4) \times (0, 4) \subset \mathbb{R}^2$, whose boundary is denoted as $\partial\Omega$. Now, f is chosen as a discontinuous function over Ω , we take

$$f(s, t) = \begin{cases} -0.8[(t - 1)^2 + (s - 1)^2] + 2t(4 - t) + 2s(4 - s), & (s, t) \in [1, 2) \times [1, 2); \\ -2[(3 - t)^2 + (s - 1)^2] + 2t(4 - t) + 2s(4 - s), & (s, t) \in [1, 2) \times [2, 3); \\ -1.2[(t - 1)^2 + (3 - s)^2] + 2t(4 - t) + 2s(4 - s), & (s, t) \in [2, 3) \times [1, 2); \\ -1.6[(3 - t)^2 + (3 - s)^2] + 2t(4 - t) + 2s(4 - s), & (s, t) \in [2, 3) \times [2, 3); \\ 2t(4 - t) + 2s(4 - s), & (s, t) \in \Omega - [1, 3) \times [1, 3). \end{cases}$$

The weak form of this model BVP can be defined as follows: find $u \in V$ such that for all $v \in V$,

$$\int_{\Omega} \nabla u \cdot \nabla v \, d\Omega = \int_{\Omega} f v \, d\Omega,$$

where $V = \{u : u \in \mathbf{H}^1(\Omega), u|_{\partial\Omega} = 0\}$, $\mathbf{H}^1(\Omega)$ is the Sobolev space that consists of the functions in $\mathbf{L}^2(\Omega)$ that possess weak and square-integrable derivatives.

In this example, $f(s, t)$ is discontinuous over Ω . We choose a C-PHT space based on the discontinuity of $f(s, t)$ as the finite element space to discretize the weak form of the BVP. The refinement is driven by the L_2 norm of error between the FEM solution and the exact solution of this BVP. By h-refinement of the mesh, we obtain the solution and adaptive refinement meshes given by the FEM shown in Fig. 15; The FEM solution of the model BVP is plotted it in Fig. 14.

5.2.2. Example 2.2

The strong form of this BVP is as follows. Find $u : \overline{\Omega} \rightarrow \mathbb{R}$ such that

$$\begin{aligned} -\Delta u &= f \quad \text{in } \Omega, \\ u &= 0 \quad \text{on } E_D, \end{aligned}$$

where Ω is a rectangular domain $(0, 2) \times (0, 1) \subset \mathbb{R}^2$, whose boundary is denoted as $\partial\Omega$, where $E_D = \partial\Omega \cup (\{1\} \times [0, 1])$.

We take the exact solution $u(s, t)$ as

$$u(s, t) = \begin{cases} s(1 - s)t(1 - t) \sin(st), & (s, t) \in [0, 1) \times [0, 1]; \\ (s - 1)(2 - s)t(1 - t) \sin(st), & (s, t) \in [1, 2) \times [0, 1] \end{cases}$$

and $f(s, t) = -\Delta u(s, t)$. It is easy to check that $u(s, t)$ is C^0 along $\{1\} \times [0, 1]$.

The weak form of this model BVP can be defined as follows: find $u \in V$ such that for all $v \in V$,

$$\int_{\Omega} \nabla u \cdot \nabla v \, d\Omega = \int_{\Omega} f v \, d\Omega,$$

where $V = \{u : u \in \mathbf{H}^1(\Omega), u|_{E_D} = 0\}$, $\mathbf{H}^1(\Omega)$ is the Sobolev space that consists of the functions in $\mathbf{L}^2(\Omega)$ that possess weak and square-integrable derivatives.

The FEM Solution By Mix orders Splines

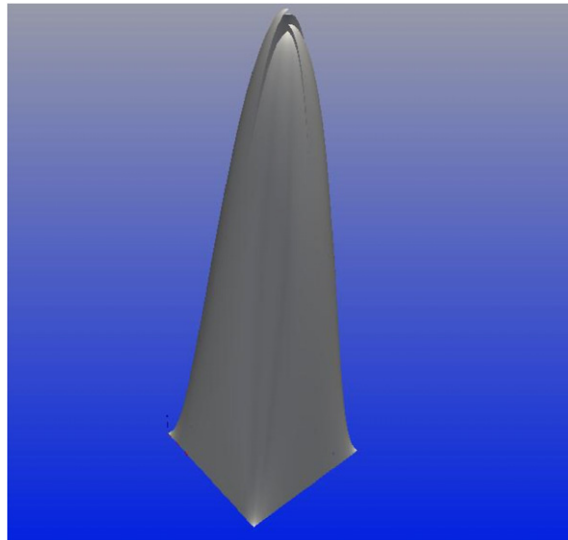


Fig. 14. The finite element solution given by C-PHT splines of the model BVP.

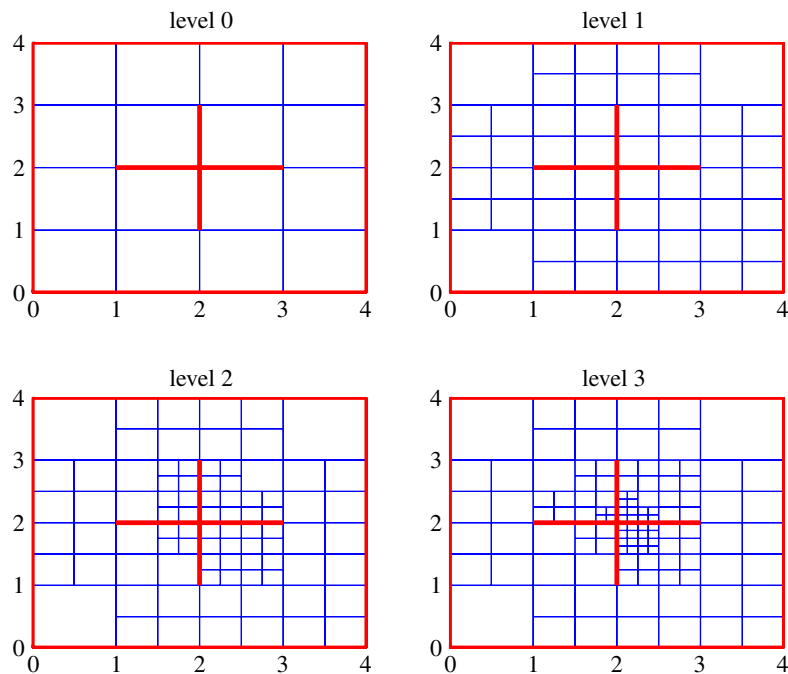


Fig. 15. The adaptive refinement meshes of the model BVP.

In contrast, we use the C-PHT space and the PHT space as finite element spaces for solving this BVP respectively. Take the tensor-product mesh $[0, 1, 2] \times [0, 1]$ as the initial mesh. For constructing the C-PHT space, if an edge of this initial mesh coincides with E_D , then it is set as a D-edge. With the same method of refinement as Example 2.1, the convergence behavior is shown in Fig. 16.

6. Conclusion and future work

In this paper, the space of spline functions with mixed orders of continuity over a T-mesh was proposed to more exactly recover data. The dimensional formula was been presented in the case of C-PHT. A set of basis functions with local

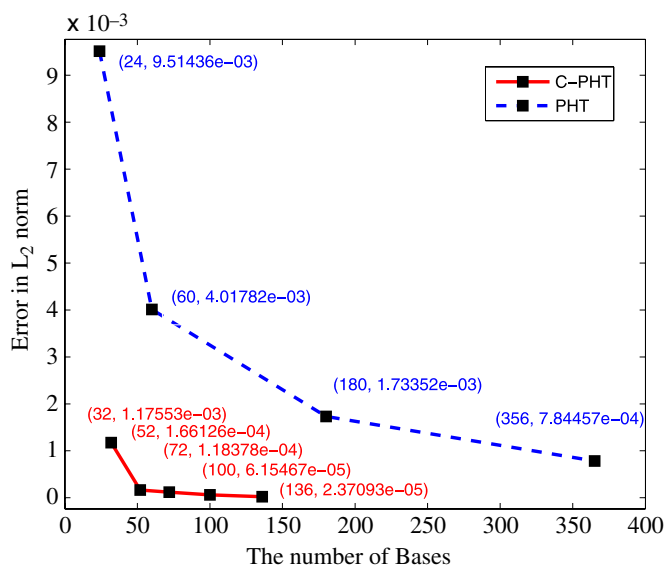


Fig. 16. The convergence behavior of FEM solutions with the help of C-PHT space and PHT space.

support, nonnegativity and partition of unity was also constructed over a hierarchical T-mesh with incomplete D-edges. As a preliminary application, C-PHT was applied to handle image data and to solve a PDE by FEM.

C-PHT splines have good potential for application in isoparametric finite element and in handling discontinuous data. However, before these applications are realized, the challenge presented by the reparameterization of a physical domain by C-PHT or PHT must be overcome which is a problem we will address in the future.

Acknowledgments

The authors are supported by a NKBRPC (2011CB302400), the NSF of China (11031007, 11371341, and 11171332), Program for New Century Excellent Talents in University (No. NCET-11-0881), the 111 Project (No. b07033), and the University Natural Science Foundation of Anhui Province (KJ2011Z317).

References

- [1] I.J. Schoenberg, Contribution to the problem of application of equidistant data by analytic functions, *Quart. Appl. Math.* 4 (1946) 45–99.
- [2] J. Ferguson, Multivariable curve interpolation, *J. ACM* 11 (1964) 221–228.
- [3] J. Stoer, R. Bulirsch, *Introduction to Numerical Analysis*, third ed., Springer, 2002.
- [4] M. Egerstedt, C. Martin, *Control Theoretic Splines: Optimal Control, Statistics, and Path Planning*, Princeton University Press, 2009.
- [5] G. Farin, *Curves and Surfaces for CAGD*, Morgan Kaufmann, 2001.
- [6] D. Forsey, R. Bartels, Hierarchical B-spline refinement, *Comput. Graph.* 22 (1988).
- [7] T.W. Sederberg, J.M. Zheng, A. Bakenov, A. Nasri, T-splines and T-NURCCs, *ACM Trans. Graph.* 22 (2003) 161–172.
- [8] J. Deng, F. Chen, Y. Feng, Dimensions of spline spaces over T-meshes, *J. Comput. Appl. Math.* 194 (2006) 267–283.
- [9] F.B. Richards, A gibbs phenomenon for spline functions, *J. Approx. Theory* 66 (1991) 344–351.
- [10] J. Walsh, A closed set of orthogonal functions, *Ann. J. Math.* 55 (1923) 5–24.
- [11] A. Haar, Zur Theorie der orthogonalen Funktionensysteme, *Math. Ann.* 69 (1910) 331–371.
- [12] Y. Feng, D.X. Qi, A sequence of piecewise orthogonal polynomials, *SIAM J. Math. Anal.* 15 (1984) 834–844.
- [13] R. Song, H. Ma, T. Wang, D.X. Qi, Complete orthogonal V-system and its applications, *Commun. Pure Appl. Anal.* 6 (2007) 853–871.
- [14] B. Cockburn, C.W. Shu, Runge-Kutta discontinuous Galerkin methods for convection-dominated problems, *J. Sci. Comput.* 16 (2001) 173–261.
- [15] R. Wang, On the analysis of multivariate splines in the case of arbitrary partition, *Sci. Sin.* (1979).
- [16] J. Deng, F. Chen, Polynomial splines over hierarchical T-meshes, *Graph. Models* 74 (2008) 76–86.
- [17] J. Deng, F. Chen, L. Jin, Dimensions of biquadratic spline spaces over T-meshes, *J. Comput. Appl. Math.* 238 (2013) 68–94.
- [18] L. Tian, F. Chen, Q. Du, Adaptive finite element methods for elliptic equations over hierarchical T-meshes, *J. Comput. Appl. Math.* 236 (2011) 878–891.
- [19] N. Nguyen-Thanh, H. Nguyen-Xuan, S. Bordas, T. Rabczuk, Isogeometric analysis using polynomial splines over hierarchical T-meshes for two dimensional elastic solids, *Comput. Methods Appl. Mech. Eng.* 200 (2011) 1892–1908.
- [20] N. Nguyen-Thanh, J. Kiendl, H. Nguyen-Xuan, R. Wüchner, K.U. Bletzinger, Y. Bazilevs, T. Rabczuk, Rotation free isogeometric thin shell analysis using PHT-splines, *Comput. Methods Appl. Mech. Eng.* 200 (2011) 3410–3424.
- [21] P. Alfeld, L.L. Schumaker, The dimension of bivariate spline spaces of smoothness r for degree $d \geq 4r + 1$, *Constr. Approx.* 3 (1987) 189–197.
- [22] M. Eck, T. DeRose, T. Duchamp, Multiresolution analysis of arbitrary meshes, in: *SIGGRAPH'95 Proceedings of the 22nd Annual Conference on Computer Graphics and Interactive Techniques* 1995, pp. 173–182.